Electronic Supplementary Information

Photocatalytic Reforming of Sugar and Glucose into H_2 over Functionalized Graphene Dots

Van-Can Nguyen,[a] Nei-Jin Ke,[a] Le Duy Nam,[a] Ba-Son Nguyen,[a,b] Yuan-Kai Xiao,[a] Yuh-Lang Lee,[a,c] Hsisheng Teng[a,c,d,*]

[a]Department of Chemical Engineering, National Cheng Kung University, Tainan 70101, Taiwan

[b]Research Center for Applied Sciences, Lac Hong University, Vietnam

[c]Hierarchical Green-Energy Materials (Hi-GEM) Research Center, National Cheng Kung University, Tainan 70101, Taiwan

[d]Center of Applied Nanomedicine, National Cheng Kung University, Tainan 70101, Taiwan

*To whom correspondence should be addressed. (E-mail): hteng@mail.ncku.edu.tw

(Fax): 886-6-2344496

Supporting information for:

(1) A sustainable carbon cycle producing solar H_2;

(2) TEM images of catalysts;

(3) Full-range and S 2p XPS spectra of catalysts;

(4) XPS spectra of SGODs;

(5) FTIR spectra of catalysts before and after reaction;

(6) PL spectra and time-resolved PL decay curves of catalysts;

(7) Fitting parameters of the PL decay curves;

(8) UPS analysis of catalysts;

(9) Solution-pH dependence of H_2 production;

(10) H_2 production over bare SNGODs under irradiation;

(11) H_2 production over Pt-deposited TiO_2 under irradiation.

1. A sustainable carbon cycle producing solar H_2

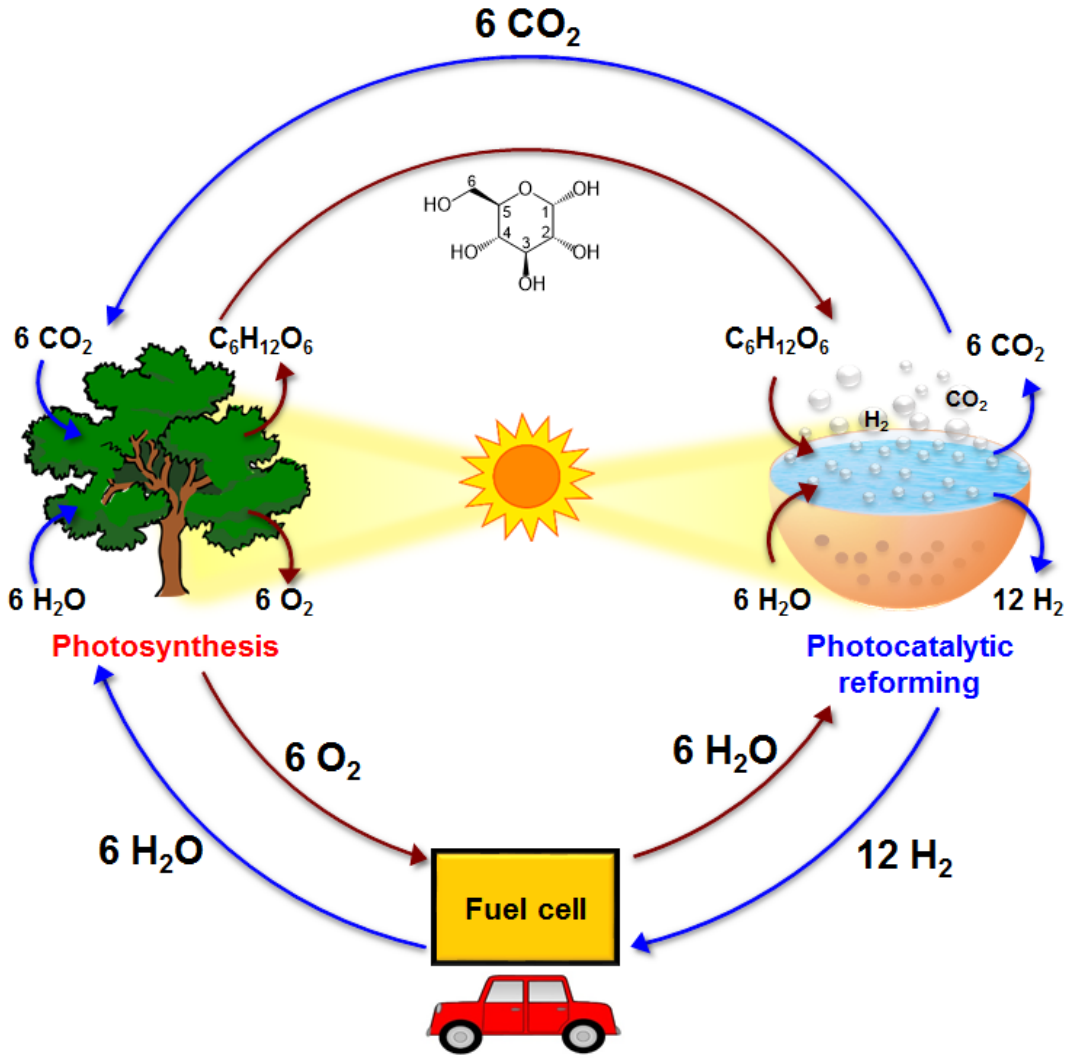

Scheme S1 Photocatalytic reforming of glucose into H_2 and photosynthesis in plants constitute a sustainable carbon cycle that produces a clean solar fuel.

2. TEM images of catalysts

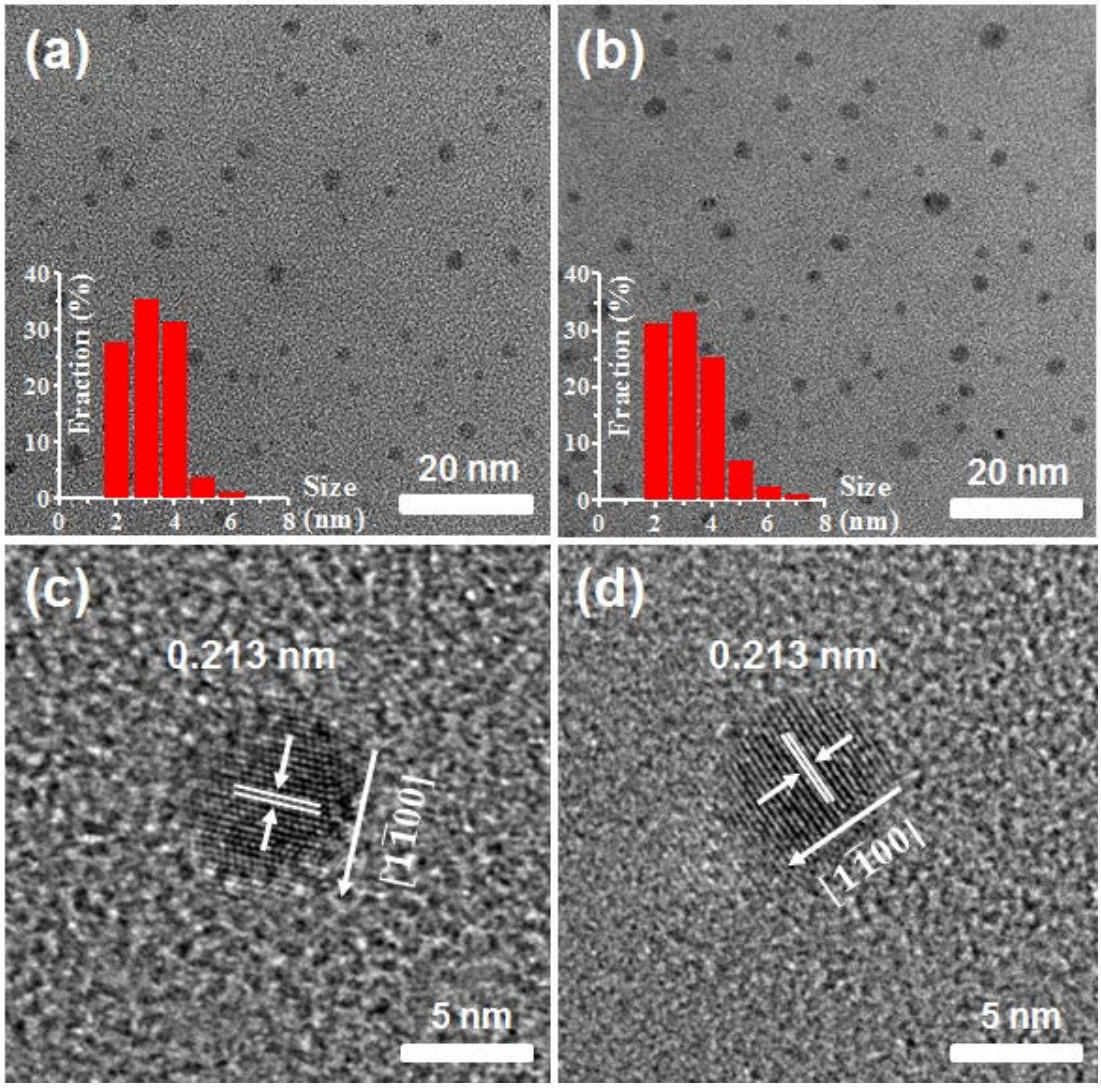

Fig. S1 TEM images of (a) NGODs and (b) SNGODs with the insets showing the histograms of size distribution. High-resolution TEM images of (c) an NGOD and (d) an SNGOD, showing the graphene $\{1\bar{1}00\}$ lattice planes with a d-spacing of 0.213 nm.

3. Full-range and S 2p XPS spectra of catalysts

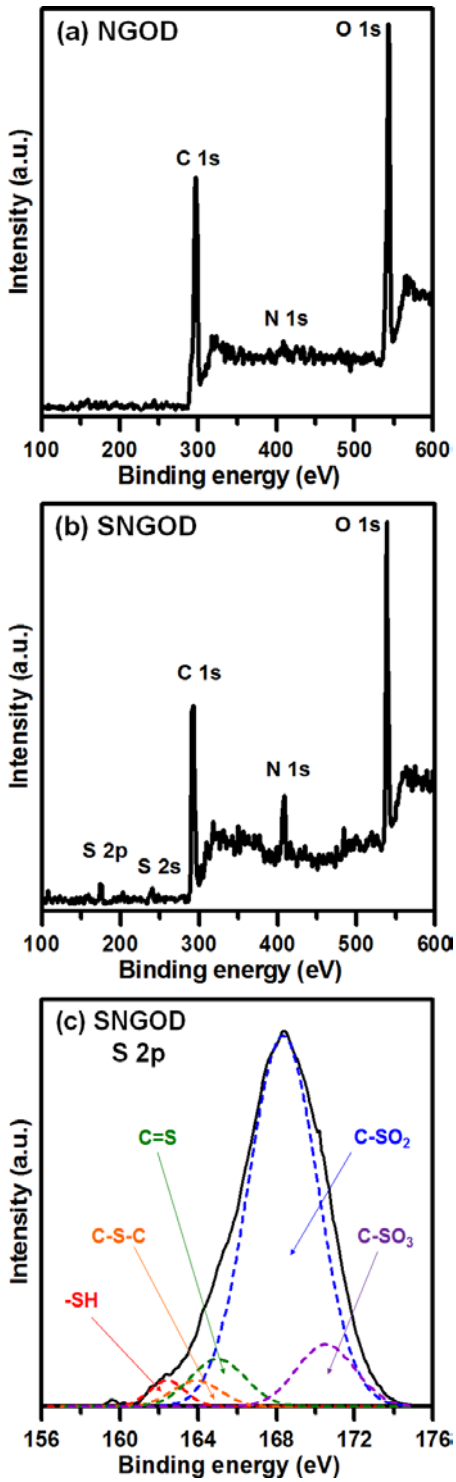

Fig. S2 Full-range XPS spectra of (a) NGODs and (b) SNGODs, and (c) S 2p XPS spectrum of SNGODs.

4. XPS spectra of SGODs

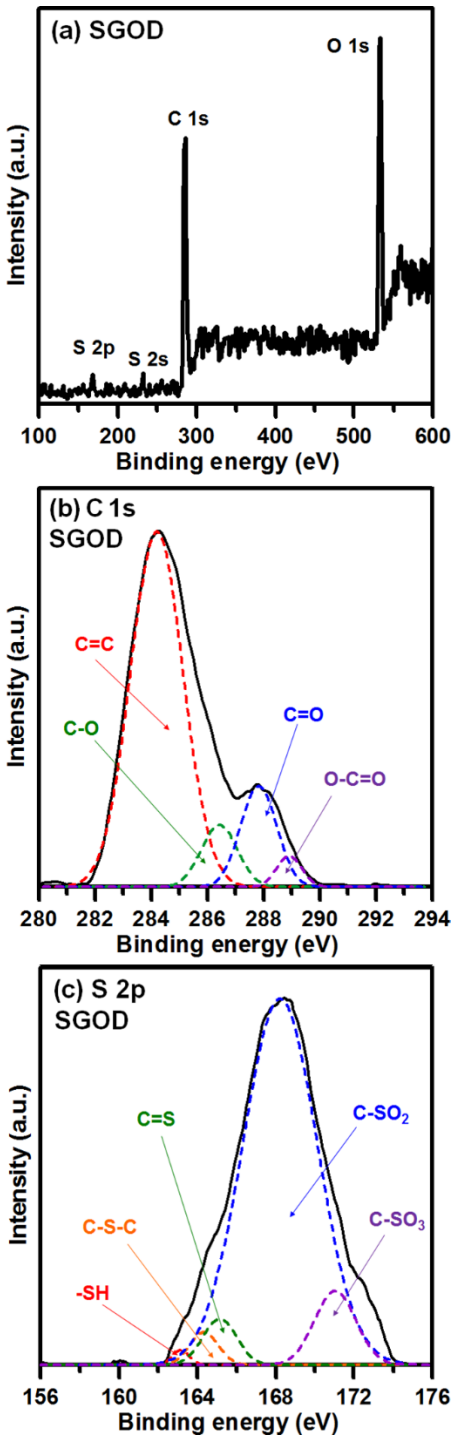

Fig. S3 XPS spectra of the SGODs: (a) full-range, (b) C 1s, and (c) S 2p.

5. FTIR spectra of catalysts before and after reaction

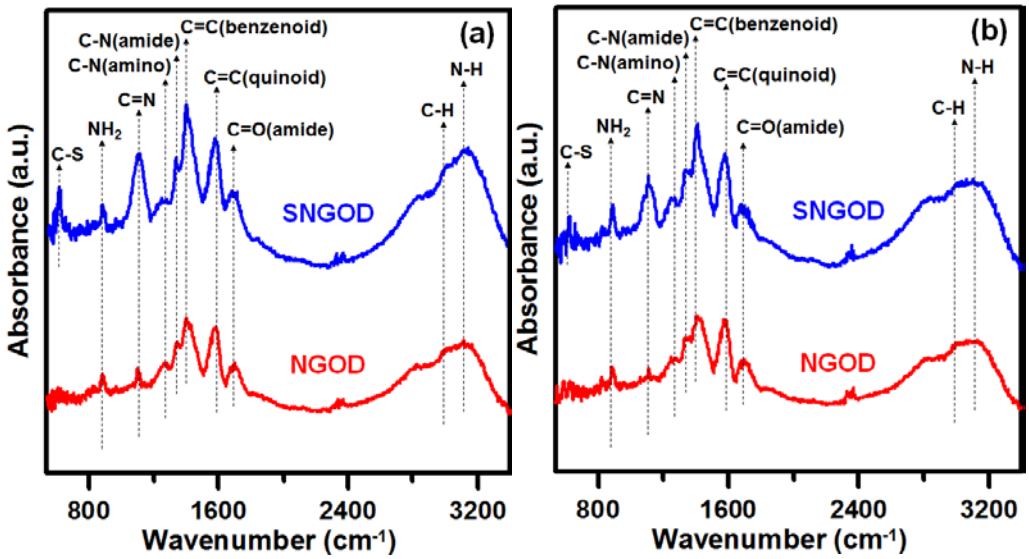

Fig. S4 FTIR spectra of the NGODs and SNGODs: (a) before-reaction and (b) after a 60-h photocatalytic reaction.

6. PL spectra and time-resolved PL decay curves of catalysts

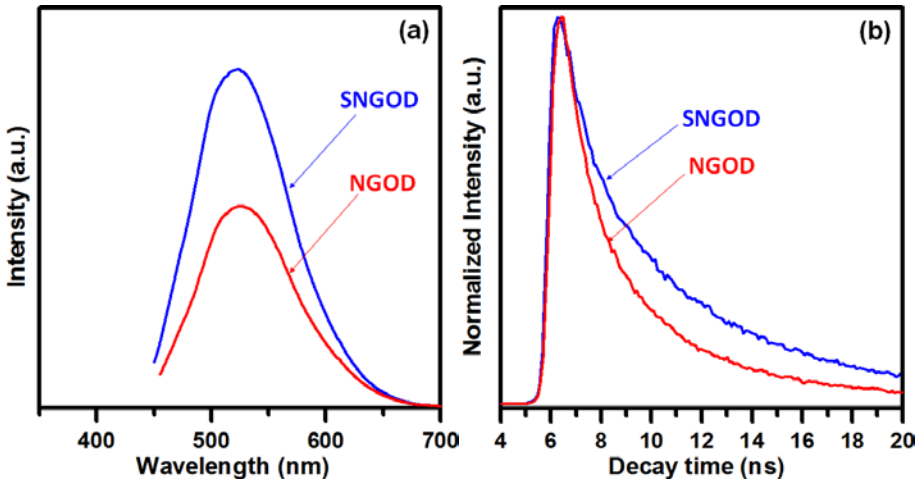

Fig. S5 (a) PL spectra of the NGOD and SNGOD aqueous suspensions under 405-nm excitation. (b) Time-resolved PL decay curves of the NGOD and SNGOD aqueous suspensions excited by a 405-nm laser.

7. Fitting parameters of the PL decay curves

Table S1. The fitting parameters of the PL decay curves (Fig. S5b) excited using a 405-nm laser. The PL emission wavelength for detection coincides with the PL peak wavelength, which is 540 nm as shown in Fig. S5a.

	τ_1 (ns)	τ_2 (ns)	A_1	A_2	τ_{ave} (ns)
NGOD	1.8	5.9	40	60	5.2
SNGOD	2.0	7.3	23	77	6.9

8. UPS analysis of catalysts

We identified the tVB level of the NGODs and SNGODs deposited on silicon substrate by using UPS equipped with He I light irradiation. The following equation was used for UPS analysis:

$$E_B + E_k + \varphi = 21.2$$

where E_B is the binding energy measured from the Fermi level (E_F), E_k is the kinetic energy of electrons, φ is the work function of the NGODs, and 21.2 eV is the energy of the He I light.

The tVB and E_F can be calculated using the following equations:

$$\text{tVB} = 21.2 - (E_{B2} - E_{B1})$$

$$E_F = 21.2 - E_{B2}$$

where E_{B2} is the secondary cutoff binding energy in the UPS spectra, in which the E_k of the excited electrons is equal to 0, and E_{B1} represents the difference between the E_F and tVB levels. **Fig. S6** shows the UPS spectra of the NGODs and SNGODs. The E_{B1} can be determined using the intercepts of the extrapolated straight lines on the abscissa at low binding energy. The E_{B2} can be estimated using the secondary cutoff values (E_k = 0 eV) in the UPS spectra, obtained from the intercepts of the extrapolated straight lines on the abscissa at high binding energy. The UPS widths are the difference between E_{B2} and E_{B1}. As presented in the above two equations, we determined the tVB level relative to the vacuum by subtracting the width of the UPS spectra ($E_{B2} - E_{B1}$) from the excitation energy (21.2 eV).

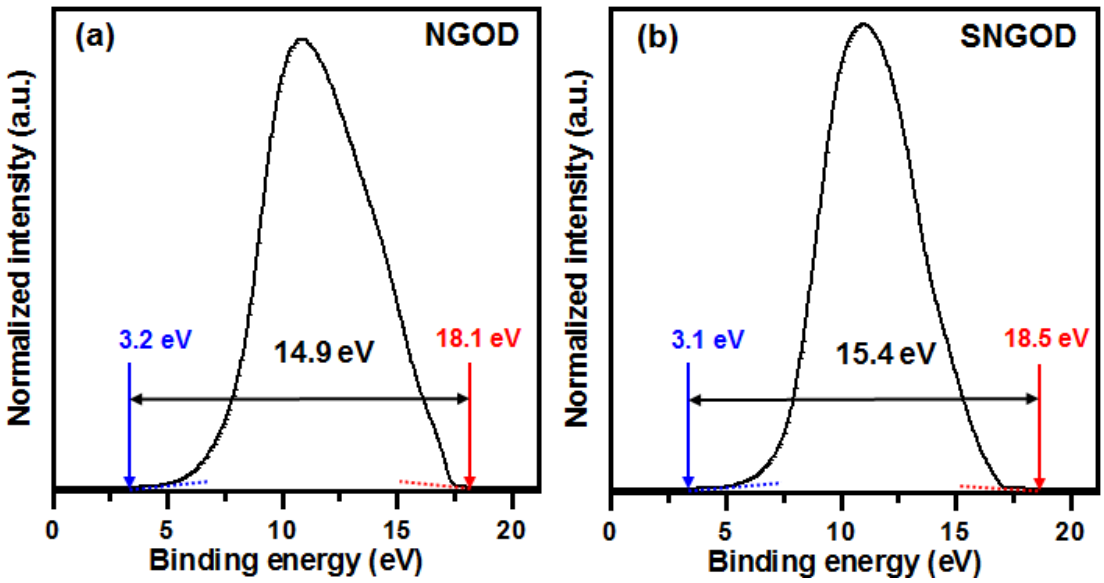

Fig. S6 UPS spectra of (a) NGODs and (b) SNGODs. The tVB energy levels with respect to the Fermi levels were determined from the intercepts of the extrapolated straight lines (blue dashed line) on the abscissa at low binding energy. The intersections of the tangent (red dashed line) with the abscissa at high binding energy give the secondary electron onset binding energy. The UPS widths (black lines) can be determined by these two intercept binding energies, and the tVB can be calculated by subtracting these widths from the excitation energy (21.2 eV).

9. Solution-pH dependence of H_2 production

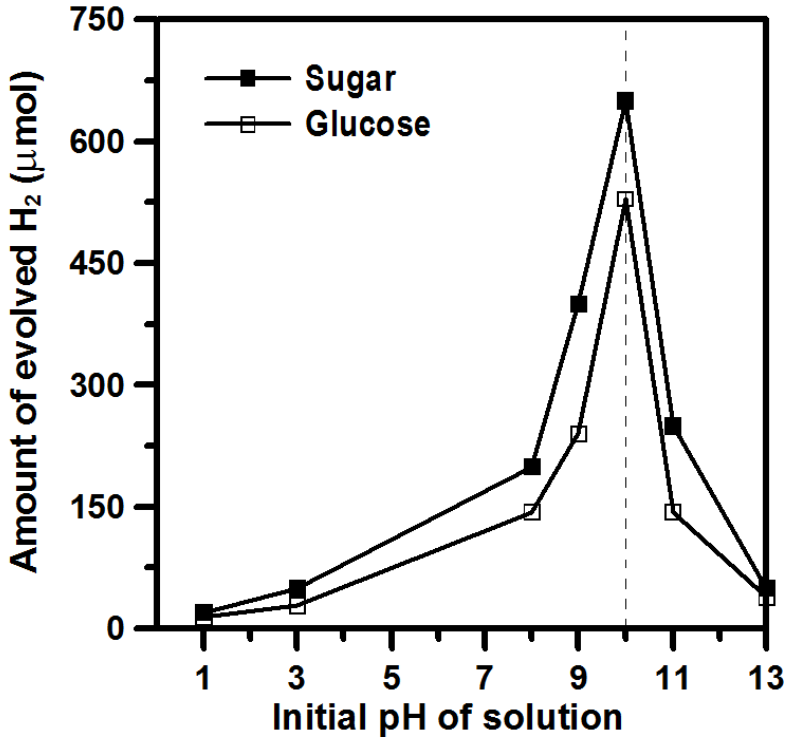

Fig. S7 The solution-pH dependence of H_2 production from photocatalytic reforming of sugar and glucose. The solutions contained 5 wt% Pt-deposited SNGODs and were irradiated by visible light (420 nm < λ < 800 nm) at an intensity of 35 mW cm^{-2} over a period of 12 h.

10. H_2 production over bare SNGODs under irradiation

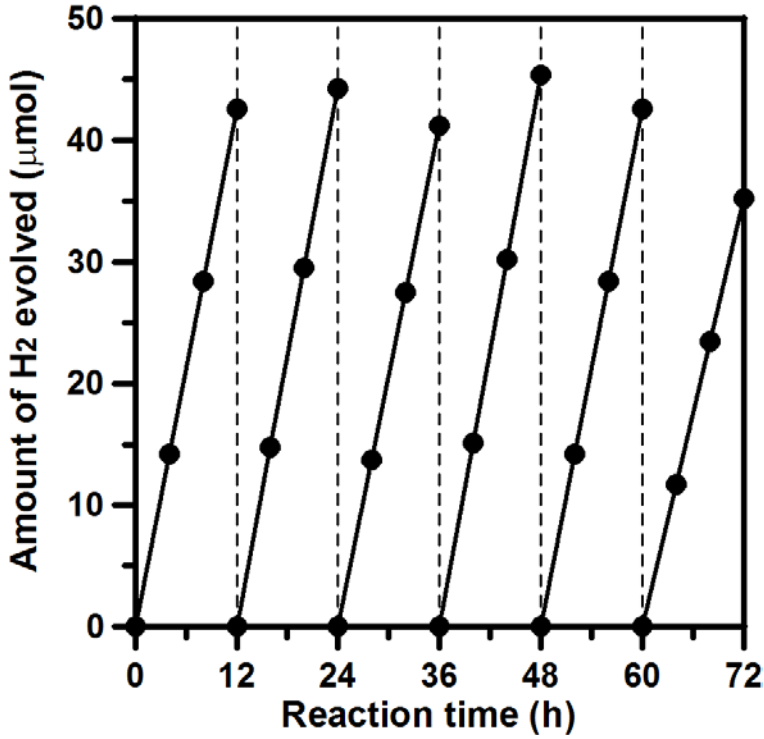

Fig. S8 Time course of H_2 production from a sugar (0.35 mol L^{-1}) aqueous solution (at pH of 10) containing bare SNGODs (0.4 g) over a period of 72 h, with several interventions for evacuating the system. The system was irradiated by visible light (420 nm < λ < 800 nm) at an intensity of 35 mW cm^{-2}.

11. H_2 production over Pt-deposited TiO_2 under irradiation

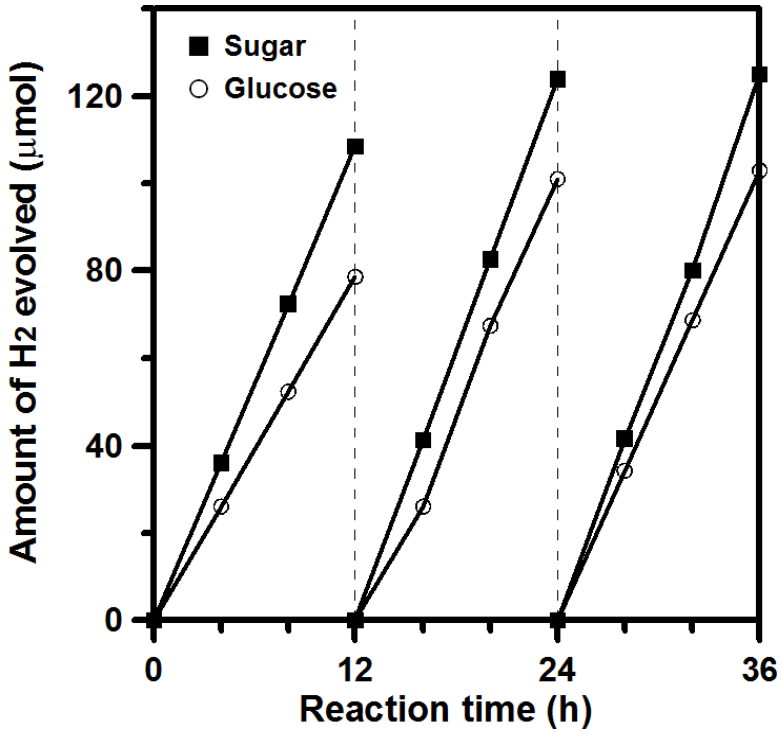

Fig. S9 The time course of H_2 production from sugar and glucose (0.35 mol L^{-1}) aqueous solutions (at pH of 10) containing 5 wt% Pt-deposited TiO_2 (0.4 g) over a period of 36 h, with several interventions for evacuating the system. The TiO_2 sample was a commercially available TiO_2 powder (P25, Degussa, Japan). The system was irradiated by visible light (420 nm < λ < 800 nm) at an intensity of 35 mW cm^{-2}.